# Supporting Information

## Direct Analysis of Doping Agents in Raw Urine Using Hydrophobic Paper Spray Mass Spectrometry

Eduardo Luiz Rossini[1, 2], Dmytro S. Kulyk[1], Emelia Ansu-Gyeabourh[1], Taghi Sahraeian[1], Helena Redigolo Pezza[2], Abraham K. Badu-Tawiah[1*]

[1]Department of Chemistry and Biochemistry, The Ohio State University, 100 West 18th Avenue, Columbus, Ohio 43210, United States
[2]Institute of Chemistry, Department of Analytical Chemistry, São Paulo State University (UNESP), R. Prof. Francisco Degni 55, P.O. Box 355, 14800-900, Araraquara, SP, Brazil

Supporting information is summarized below:

## 1. Paper silanization

The paper treatment with trichlorosilane derivative was conducted via vapor-phase deposition. Typically, 0.5 mL of thichlorosilane derivate in a vial was put on the bottom of the desiccator and the paper triangles were located on the desiccator plate. Under reduced pressure (20 torr) the partial pressure of the thichlorosilane derivative enriched the vapor phase with that organosilane component (Figure S1a). The moisture present in the paper and in the desiccator catalyzed the polymerization between the thichlorosilane derivative, in the form of organosilanol ($RSi(OH)_3$), and the hydroxyl groups present in the paper surface releasing water, molecule takes part in the polymerization, plus hydrochloric acid (Figure S1b). The reaction was stopped when the atmospheric pressure was restored and the hydrophobic paper triangles were removed from the desiccator. For all experiments, the paper triangles were cut before silanization.

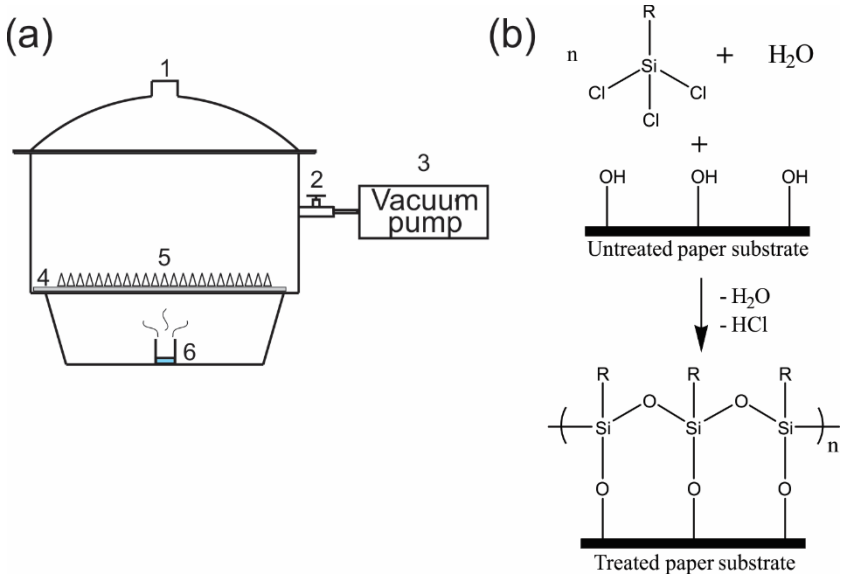


**Figure S1.** (a) Schematic illustration of the setup used for vapor-phase silanization. 1. Desiccator; 2. Valve; 3. Vacuum pump system; 4. Desiccator plate; 5. Paper triangles; 6. Organosilane. (b) Paper modification through silanization of surface hydroxyl groups using trichlorosilane vapor to create a hydrophobic layer onto the paper.

## 2. Surface energy estimation via bracketing

The surface energy of a substrate is the quantitative representation of its hydrophobicity. The surface energies of the paper triangles treated with TCMS and TCTFPS were estimated via bracketing method. Complete wetting happens only when the surface tension of the wetting liquid is less than the critical energy of the surface. The central idea in the bracketing is if a liquid drop wets a surface, the surface energy of the wetted substrate is lower than the dry substrate. Consequently, for the paper surface energy estimation, if the paper is wetted through by a drop of a specific liquid, its critical surface energy is higher than the surface tension of that liquid; otherwise, if the paper is not wetted through by the drop of a specific liquid, then its critical surface energy is lower than the surface tension of that liquid[1].

Different pure solvents and mixtures of water and acetonitrile were used to estimate the surface energy of hydrophobic paper by bracketing (Table S1). A 10 µL droplet of solvent was cast onto the different papers, initiating from the solvent with higher to the solvent with lower surface tension. This procedure was repeated for the papers treated with different treatment times and different treatment reagents. Table S2 indicates the results of the wettability study. Papers treated for 15 to 240 min with TCMS have surface energy between 43.12-47.3 mN $m^{-1}$, while papers treated for 15 to 240 min with TCTFPS have surface energy between 43.54-49.39 mN $m^{-1}$. As we expected, longer silanization times decrease the surface energy of the paper, increasing its hydrophobicity. Additionally, paper modified with TCMS have lower surface energy, or are more hydrophobic, than paper functionalized with TCTFPS.

**Table S1.** Surface tension of different solvents and mixtures of different molar fraction of water and acetonitrile.

| Solvent | Surface tension (mN $m^{-1}$)[2] | $x_{ACN}$ | $x_{H2O}$ |
|---|---|---|---|
| 1 | 62.36 | 0.0149 | 0.9851 |
| 2 | 55.92 | 0.0298 | 0.9702 |
| 3 | 49.39 | 0.0576 | 0.9484 |
| Ethylene Glycol | 47.3 | - | - |
| DMSO | 43.54 | - | - |
| Quinoline | 43.12 | - | - |
| 4 | 40.54 | 0.095 | 0.905 |
| 5 | 37.97 | 0.1227 | 0.8773 |
| Cyclohexanol | 34.4 | - | - |
| 6 | 32.92 | 0.2541 | 0.7459 |
| 7 | 31.68 | 0.3959 | 0.6041 |
| 8 | 31.45 | 0.4851 | 0.5149 |
| 9 | 30.95 | 0.5913 | 0.4087 |
| 10 | 28.66 | 1 | 0 |

**Table S2.** Surface energy estimation of papers treated for different times using TCMS and TCTFPS by bracketing method.

| Treatment time (min) | Surface energy (mN $m^{-1}$) | |
|---|---|---|
| | **TCMS treated paper** | **TCTFPS treated paper** |
| 15 | 43.54 – 47.3 | 47.3 – 49.39 |
| 30 | 43.54 – 47.3 | 47.3 – 49.39 |
| 60 | 43.12 – 43.54 | 43.54 – 47.3 |
| 120 | 43.12 – 43.54 | 43.54 – 47.3 |
| 240 | 43.12 – 43.54 | 43.54 – 47.3 |

## 3. Central composite design for optimization of the tube lens voltage and capillary temperature

A central composite design was used to optimize the tube lens voltage and capillary temperature for adduct formation, in-source fragmentation and ionized molecular ion intensity. Table S3 shows the central composite design matrix for furosemide and hydrochlorothiazide. Table S4 shows the central composite design matrix for trenbolone and for clenbuterol. The combinations of the selected factors resulted in ten experiments, carried out in triplicate.

**Table S3** Central composite design matrices for the furosemide and hydrochlorothiazide. The codified levels of the factors are in front of the real values used for the design.

| Experiment | Factors | | | |
|---|---|---|---|---|
| | Furosemide | | Hydrochlorothiazide | |
| | Capillary temperature (°C) | Tube lens voltage (V) | Capillary temperature (°C) | Tube lens voltage (V) |
| **1** | 125 (-1) | -175 (-1) | 150 (-1) | -175(-1) |
| **2** | 125 (-1) | -100 (+1) | 150 (-1) | -100 (+1) |
| **3** | 250 (+1) | -175(-1) | 275 (+1) | -175(-1) |
| **4** | 250 (+1) | -100 (+1) | 275 (+1) | -100 (+1) |
| **5** | 100 (-√2) | -140 (0) | 125 (-√2) | -140 (0) |
| **6** | 275 (+√2) | -140 (0) | 300 (+√2) | -140 (0) |
| **7** | 190 (0) | -190 (+√2) | 215 (0) | -190 (+√2) |
| **8** | 190 (0) | -85 (-√2) | 215 (0) | -85 (-√2) |
| **9** | 190 (0) | -140 (0) | 215 (0) | -140 (0) |
| **10** | 190 (0) | -140 (0) | 215 (0) | -140 (0) |

**Table S4** Central composite design matrix for the trenbolone and clenbuterol. The codified levels of the factors are in front of real values used for the design.

| Experiment | Factor | |
|---|---|---|
| | **Capillary temperature (°C)** | **Tube lens voltage (V)** |
| **1** | 200 (-1) | 50 (-1) |
| **2** | 200 (-1) | 150 (+1) |
| **3** | 300 (+1) | 50 (-1) |
| **4** | 300 (+1) | 150 (+1) |
| **5** | 180 ($-\sqrt{2}$) | 100 (0) |
| **6** | 320 ($+\sqrt{2}$) | 100 (0) |
| **7** | 250 (0) | 30 ($-\sqrt{2}$) |
| **8** | 250 (0) | 170 ($+\sqrt{2}$) |
| **9** | 250 (0) | 100 (0) |
| **10** | 250 (0) | 100 (0) |

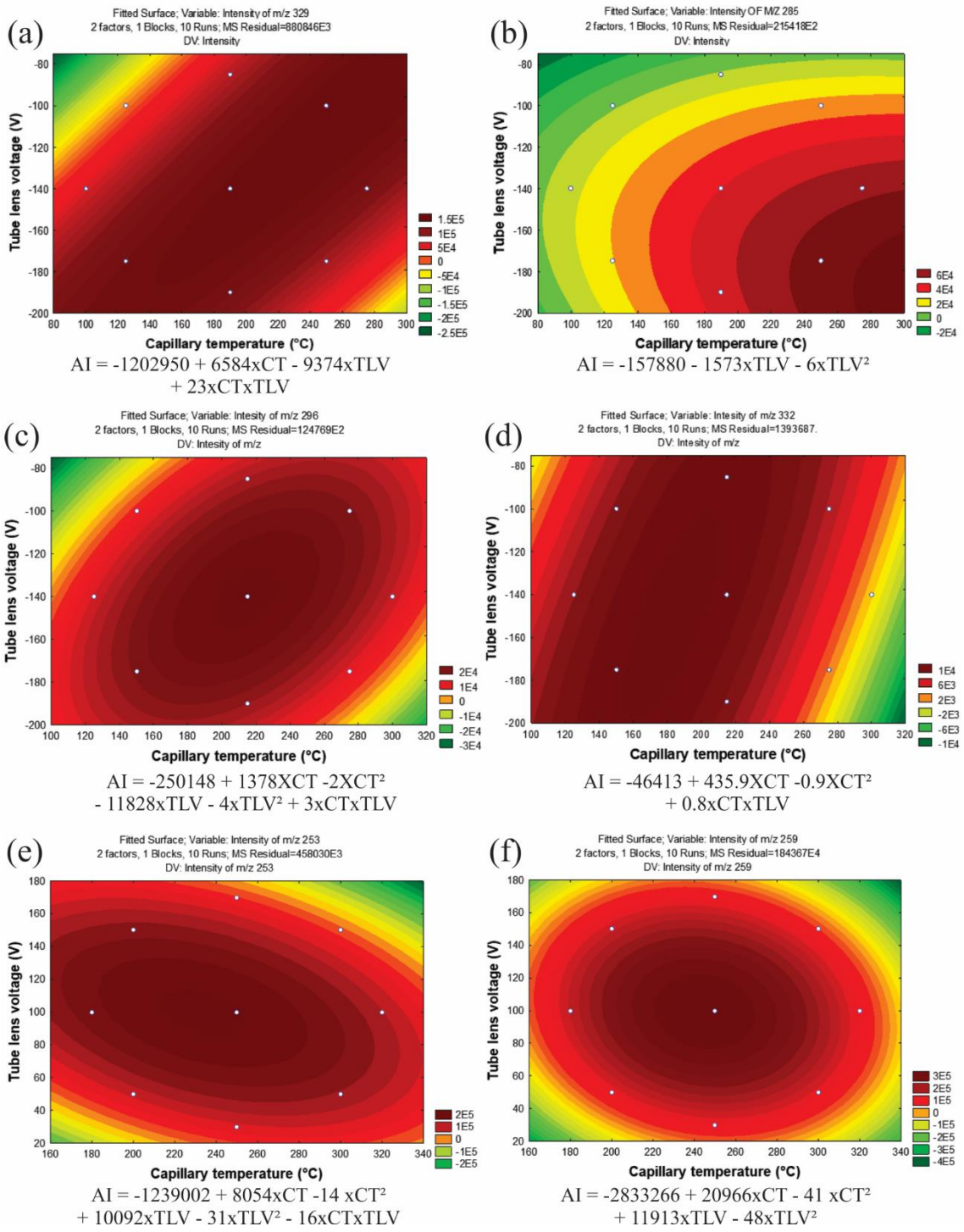


**Figure S2.** Projection of the central composite design response surfaces obtained for absolute intensity (AI) as a function of tube lens voltage (TLV) and capillary temperature (CT) for (a) deprotonated furosemide ion ($[M-H]^-$ at *m/z* 329), (b) furosemide in-source fragment product ($[M-CO_2-H]^-$ at *m/z* 285), (c) deprotonated hydrochlorothiazide ion ($[M-H]^-$ at *m/z* 296), (d) hydrochlorothiazide chlorine adduct ($[M+Cl]^-$ at *m/z* 332), (e) $MS^2$ product ion for protonated trenbolone ion (*m/z* 271 → 253), and (f) $MS^2$ product ion for protonated clenbuterol ion (*m/z* 277 → 259).

## 4. Physical chemical properties of the solvents

Table S5 describes the surface tension, dielectric constant and chemical properties for acetone, acetonitrile, ethyl acetate, methanol, and water.

**Table S5** Physical chemical properties of the solvents.

| **Solvent** | **Surface tension at 25°C (mN $m^{-1}$)**[3] | **Dielectric constant at 25°C**[3] | **Relative polarity** [4] |
|---|---|---|---|
| Acetone | 22.71 | 21.01 | 0.355 |
| Acetonitrile | 28.66 | 36.64 | 0.460 |
| Ethyl acetate | 25.13 | 6.081 | 0.228 |
| Methanol | 23.47 | 33.0 | 0.762 |
| Water | 72.06 | 80.1 | 1.000 |

## 5. Spray voltage

Dependence of the signal intensities when different spray voltages were applied to the paper triangle, using ethyl acetate as spray solvent for both positive- and negative-ion modes.

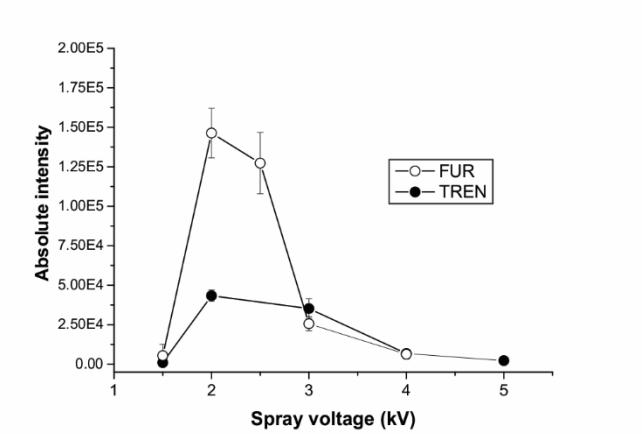


**Figure S3.** Effect of the spray voltage on signal intensity. Trenbolone (black circle - 500 ng $mL^{-1}$) was monitored in $MS^2$ experiment using the most abundant product ion at *m/z* 253, in positive-ion mode, and furosemide (white circle – 12.5 µg $mL^{-1}$) was monitored in $MS^2$ experiment using the most abundant product ion at *m/z* 285, in negative-ion mode. Error bars represent the standard deviation of analyses for three replicates with independent hydrophobic paper triangles.

## 6. Analytical curves for trenbolone, clenbuterol, furosemide and hydrochlorothiazide

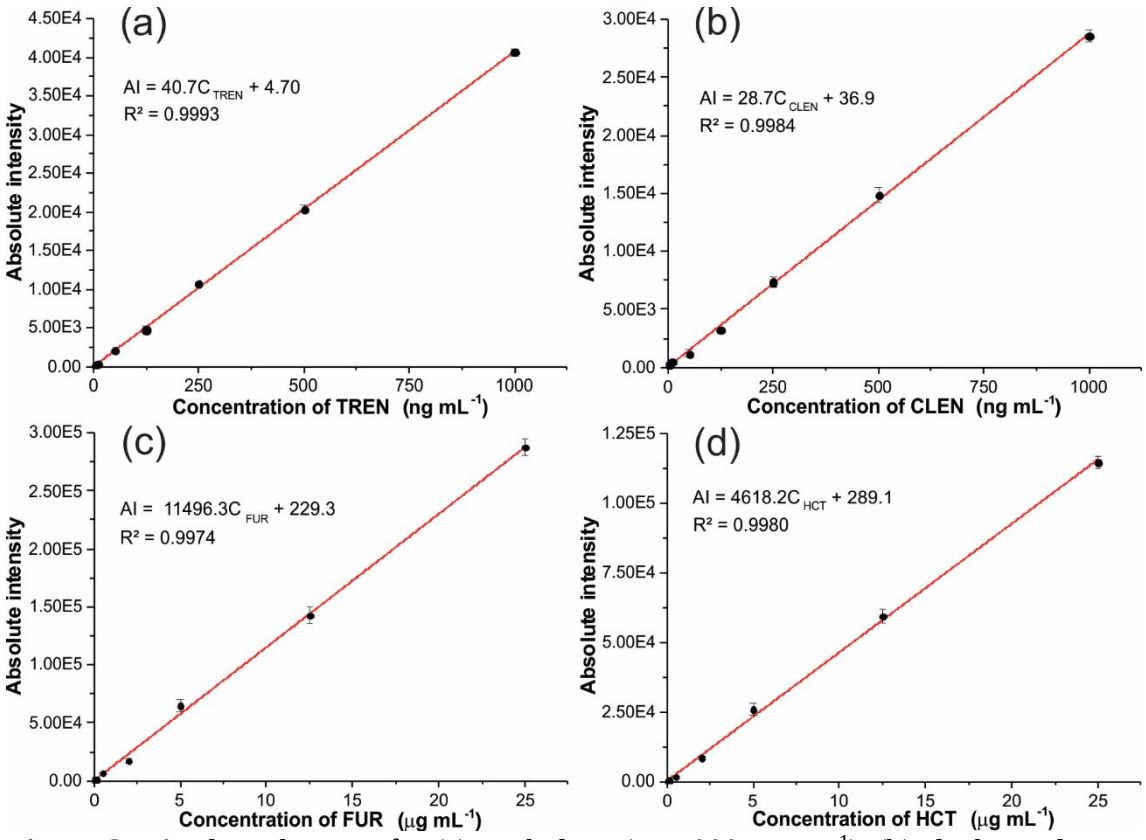


**Figure S4.** Analytical curves for (a) trenbolone (5 - 1000 ng $mL^{-1}$), (b) clenbuterol (1 - 1000 ng $mL^{-1}$), (c) furosemide (50 - 25 x $10^3$ ng $mL^{-1}$), and (d) hydrochlorothiazide (50 - 25 x $10^3$ ng $mL^{-1}$). Quantification of each analyte was performed by analyzing the following product ion from each compound: trenbolone (*m/z* 271 → 227), clenbuterol (*m/z* 277 → 203), furosemide (*m/z* 329 → 285), and hydrochlorothiazide (*m/z* 296 → 269). Error bars represent the standard deviation of analyses for three replicates with independent hydrophobic paper triangles.

## 7. Figures of merit for trenbolone, clenbuterol, furosemide and hydrochlorothiazide.

**Table S6.** Regression data, linear range, LOD and LOQ for trenbolone, clenbuterol, furosemide and hydrochlorothiazide in urine samples using hydrophobic PS-MS.

| Analyte | Linear range (ng $mL^{-1}$) | Regression equation | $R^2$ | LOD (LOQ) (ng $mL^{-1}$) | LOD (LOQ) (pg) |
|---|---|---|---|---|---|
| Trenbolone | 5 – 1000 | AI = 40.7C + 4.70 | 0.9993 | 0.21 (0.42) | 1.27 (2.49) |
| Clenbuterol | 1 – 1000 | AI = 28.7C + 36.9 | 0.9984 | 0.041 (0.076) | 0.25 (0.46) |
| Furosemide | 50 – 25 x $10^3$ | AI = 11496.3C + 229.3 | 0.9974 | 0.82 (1.65) | 4.89 (9.89) |
| Hydrochloro-thiazide | 50 – 25 x $10^3$ | AI = 4618.2C + 289.1 | 0.9980 | 0.058 (0.12) | 0.35 (0.71) |

## 8. Comparison of methods for quantification of trenbolone, clenbuterol, furosemide and hydrochlorothiazide

**Table S7.** Parameters comparison of the current work and previously reported methodologies for determination of trenbolone and clenbuterol

| Doping Substance | Method | Sample preparation | LOD (ng mL$^{-1}$) | LOQ (ng mL$^{-1}$) | Reference |
|---|---|---|---|---|---|
| Trenbolone | CBS-MS[1] | Automated extraction/rinsing using a 96-well plate | - | 10 | [5] |
| | LC-MS | LLE[2] | 0.1 | - | [6] |
| | LC-MS | LLE | 0.05 | - | [7] |
| | LC-MS | SPE[3] and LLE | 1 | - | [8] |
| | GC-MS | LLE and derivatization | 1 | - | [9] |
| | LC-MS | LLE | 10 | - | [10] |
| | LC-MS | Automated SPME[4] | - | 5 | [11] |
| | LC-MS | SPE and LLE | 0.1 | - | [12] |
| | PS-MS | - | 0.21 | 0.42 | This work |
| Clenbuterol | CBS-MS | Automated SLE[5] using a 96-well plate | - | 2.5 | [5] |
| | LC-MS | SPE and LLE | 0.1 | - | [8] |
| | GC-MS | LLE and derivatization | 0.04 | - | [9] |
| | LC-MS | LLE | 0.4 | - | [10] |
| | LC-MS | Automated SPME | - | 15 | [11] |
| | LC-AD | Dilution | 40 | - | [13] |
| | GC-MS | LLE and derivatization | 0.05 | - | [14] |
| | GC-MS | LLE and derivatization | 0.1 | - | [15] |
| | OPP-API-MS[6] | Bio-SPME | 0.03 | 0.1 | [16] |
| | LC-MS | SPE | 0.044 | 0.15 | [17] |
| | GC-MS | LLE and derivatization | 0.03 | - | [18] |
| | PS-MS | - | 0.041 | 0.076 | This work |

[1]CBS-MS = Coated blade spray-mass spectrometry.

[2]LLE = Liquid-liquid extraction.

[3]SPE = Solid-phase extraction.

[4]SPME = Solid-phase microextraction.

[5]SLE = Solid-liquid extraction.

[6]OPP-API-MS = Open port probe-ambient pressure ionization-mass spectrometry.

**Table S8.** Comparison of parameters of the current work and previously reported methodologies for determination of furosemide and hydrochlorothiazide

| Doping Substance | Method | Sample preparation | LOD (ng $mL^{-1}$) | LOQ (ng $mL^{-1}$) | Reference |
|---|---|---|---|---|---|
| Furosemide | LC-MS | LLE[1] | 2 | - | [7] |
| | LC-MS | LLE | 12.5 | - | [10] |
| | LC-MS | Automated SPME[2] | - | 10 | [11] |
| | LC-MS | SPE[3] | 0.85 | 2.8 | [17] |
| | LC-MS | SPE | 25.0 | - | [19] |
| | LC-MS | Online SPE | 5 | - | [20] |
| | Fluorescence | Centrifugation | 6 | - | [21] |
| | Spectrophotometric | LLE | 110 | 280 | [22] |
| | GC-MS | LLE and derivatization | 50 | - | [23] |
| | PS-MS | - | 0.82 | 1.65 | This work |
| Hydrochloro-thizaide | LC-MS | LLE | 2 | - | [7] |
| | LC-MS | LLE | 25 | - | [10] |
| | LC-MS | SPE | 0.24 | 0.80 | [17] |
| | LC-MS | SPE | 50 | - | [19] |
| | LC-MS | Online SPE | 1 | - | [20] |
| | GC-MS | LLE and derivatization | 50 | - | [23] |
| | LC-UV | MMIPs-d-SPE[4] | 0.75 | 2.2 | [24] |
| | Voltammetry | Centrifugation and filtration | 6 | - | [25] |
| | LC-UV | Dilution | 4 | 12 | [26] |
| | PS-MS | - | 0.058 | 0.12 | This work |

[1]LLE = Liquid-liquid extraction.

[2]SPME = Solid-phase microextraction.

[3]SPE = Solid-phase extraction.

[4]MMIPs-d-SPE = Superparamagnetic molecularly imprinted polymers-dispersive solid phase extraction.

## References


(1) Swiner, D. J.; Jackson, S.; Durisek, G. R.; Walsh, B. K.; Kouatli, Y.; Badu-Tawiah, A. K. Microsampling with Cotton Thread: Storage and Ultra-Sensitive Analysis by Thread Spray Mass Spectrometry. *Anal. Chim. Acta* **2019**, *1082*, 98–105.

(2) Rafati, A. A.; Bagheri, A.; Najafi, M. Experimental Data and Correlation of Surface Tensions of the Binary and Ternary Systems of Water + Acetonitrile + 2-Propanol at 298.15 K and Atmospheric Pressure. *J. Chem. Eng. Data* **2010**, *55* (9), 4039–4043.

(3) *CRC Handbook of Chemistry and Physics*, 100th ed.; Rumble, J. R., Ed.; CRC Press: Boca Raton, 2019.

(4) Reichardt, C.; Welton, T. *Solvents and Solvent Efects in Organic Chemistry*, 4th ed.; Wiley-VCH: Weinheim, 2011.

(5) Kasperkiewicz, A.; Gómez-Ríos, G. A.; Hein, D.; Pawliszyn, J. Breaching the 10 Second Barrier of Total Analysis Time for Complex Matrices via Automated Coated Blade Spray. *Anal. Chem.* **2019**, *91* (20), 13039–13046.

(6) He, G.; Wu, Y.; Lu, J. Doping Control Analysis of 13 Steroids and Structural-like Analytes in Human Urine Using Quadrupole-Orbitrap LC–MS/MS with Parallel Reaction Monitoring (PRM) Mode. *Steroids* **2018**, *131* (August 2017), 1–6.

(7) Abushareeda, W.; Vonaparti, A.; Saad, K. Al; Almansoori, M.; Meloug, M.; Saleh, A.; Aguilera, R.; Angelis, Y.; Horvatovich, P. L.; Lommen, A.; et al. High Resolution Full Scan Liquid Chromatography Mass Spectrometry Comprehensive Screening in Sports Antidoping Urine Analysis. *J. Pharm. Biomed. Anal.* **2018**, *151*, 10–24.

(8) Cha, E.; Kim, S.; Kim, H. W.; Lee, K. M.; Kim, H. J.; Kwon, O. S.; Lee, J. Relationships between Structure, Ionization Profile and Sensitivity of Exogenous Anabolic Steroids under Electrospray Ionization and Analysis in Human Urine Using Liquid Chromatography-Tandem Mass Spectrometry. *Biomed. Chromatogr.* **2016**, *30* (4), 555–565.

(9) Gansbeke, W. Van; Polet, M.; Hooghe, F.; Devos, C.; Eenoo, P. Van. Improved Sensitivity by Use of Gas Chromatography-Positive Chemical Ionization Triple Quadrupole Mass Spectrometry for the Analysis of Drug Related Substances. *J. Chromatogr. B Anal. Technol. Biomed. Life Sci.* **2015**, *1001*, 221–240.

(10) Jeong, E. S.; Kim, S. H.; Cha, E. J.; Lee, K. M.; Kim, H. J.; Lee, S. W.; Kwon, O. S.; Lee, J. Simultaneous Analysis of 210 Prohibited Substances in Human Urine by Ultrafast Liquid Chromatography/Tandem Mass Spectrometry in Doping Control. *Rapid Commun. Mass Spectrom.* **2015**, *29* (4), 367–384.

(11) Boyaci, E.; Gorynski, K.; Rodriguez-Lafuente, A.; Bojko, B.; Pawliszyn, J. Introduction of Solid-Phase Microextraction as a High-Throughput Sample Preparation Tool in Laboratory Analysis of Prohibited Substances. *Anal. Chim. Acta* **2014**, *809*, 69–81.

(12) Kim, S. H.; Cha, E. J.; Lee, K. M.; Kim, H. J.; Kwon, O. S.; Lee, J. Simultaneous Ionization and Analysis of 84 Anabolic Androgenic Steroids in Human Urine Using Liquid Chromatography-Silver Ion Coordination Ionspray/Triple-Quadrupole Mass Spectrometry. *Drug Test. Anal.* **2014**, *6* (11–12), 1174–1185.

(13) Lomae, A.; Nantaphol, S.; Kondo, T.; Chailapakul, O.; Siangproh, W.; Panchompoo, J. Simultaneous Determination of β-Agonists by UHPLC Coupled with Electrochemical Detection Based on Palladium Nanoparticles Modified BDD Electrode. *J. Electroanal. Chem.* **2019**, *840*, 439–448.

(14) Abushareeda, W.; Tienstra, M.; Lommen, A.; Blokland, M.; Sterk, S.; Kraiem, S.;

Horvatovich, P.; Nielen, M.; Al-Maadheed, M.; Georgakopoulos, C. Comparison of Gas Chromatography/Quadrupole Time-of-Flight and Quadrupole Orbitrap Mass Spectrometry in Anti-Doping Analysis: I. Detection of Anabolic-Androgenic Steroids. *Rapid Commun. Mass Spectrom.* **2018**, *32* (23), 2055–2064.

(15) Abushareeda, W.; Lyris, E.; Kraiem, S.; Wahaibi, A. Al; Alyazidi, S.; Dbes, N.; Lommen, A.; Nielen, M.; Horvatovich, P. L.; Alsayrafi, M.; et al. Gas Chromatographic Quadrupole Time-of-Flight Full Scan High Resolution Mass Spectrometric Screening of Human Urine in Antidoping Analysis. *J. Chromatogr. B Anal. Technol. Biomed. Life Sci.* **2017**, *1063*, 74–83.

(16) Gómez-Ríos, G. A.; Liu, C.; Tascon, M.; Reyes-Garcés, N.; Arnold, D. W.; Covey, T. R.; Pawliszyn, J. Open Port Probe Sampling Interface for the Direct Coupling of Biocompatible Solid-Phase Microextraction to Atmospheric Pressure Ionization Mass Spectrometry. *Anal. Chem.* **2017**, *89* (7), 3805–3809.

(17) Domínguez-Romero, J. C.; García-Reyes, J. F.; Lara-Ortega, F. J.; Molina-Díaz, A. Screening and Confirmation Capabilities of Liquid Chromatography-Time-of-Flight Mass Spectrometry for the Determination of 200 Multiclass Sport Drugs in Urine. *Talanta* **2015**, *134*, 74–88.

(18) Yang, S.; Liu, X.; Xing, Y.; Zhang, D.; Wang, S.; Wang, X.; Xu, Y.; Wu, M.; He, Z.; Zhao, J. Detection of Clenbuterol at Trace Levels in Doping Analysis Using Different Gas Chromatographic-Mass Spectrometric Techniques. *J. Chromatogr. Sci.* **2013**, *51* (5), 436–445.

(19) Sardela, V. F.; Martucci, M. E. P.; de Araújo, A. L. D.; Leal, E. C.; Oliveira, D. S.; Carneiro, G. R. A.; Deventer, K.; Van Eenoo, P.; Pereira, H. M. G.; Aquino Neto, F. R. Comprehensive Analysis by Liquid Chromatography Q-Orbitrap Mass Spectrometry: Fast Screening of Peptides and Organic Molecules. *J. Mass Spectrom.* **2018**, *53* (6), 476–503.

(20) De Wilde, L.; Roels, K.; Polet, M.; Van Eenoo, P.; Deventer, K. Identification and Confirmation of Diuretics and Masking Agents in Urine by Turbulent Flow Online Solid-Phase Extraction Coupled with Liquid Chromatography-Triple Quadrupole Mass Spectrometry for Doping Control. *J. Chromatogr. A* **2018**, *1579*, 31–40.

(21) Tsyrulneva, I.; Zaporozhets, O. Simple and Rapid Determination of Diuretics by Luminescent Method. *Pharmacol. & Pharm.* **2013**, *04* (07), 520–527.

(22) Tharpa, K.; Basavaiah, K.; Vinay, K. B. Use of a Diazocoupling Reaction for Sensitive and Selective Spectrophotometeric Determination of Furosemide in Spiked Human Urine and Pharmaceuticals. *Chem. Pap.* **2010**, *64* (4), 415–423.

(23) Zaporozhets, O.; Tsyrulneva, I.; Ischenko, M. Determination of 8 Diuretics and Probenecid in Human Urine by Gas Chromatography-Mass Spectrometry: Confirmation Procedure. *Am. J. Anal. Chem.* **2012**, *03* (04), 320–327.

(24) Arabi, M.; Ghaedi, M.; Ostovan, A. Development of a Lower Toxic Approach Based on Green Synthesis of Water-Compatible Molecularly Imprinted Nanoparticles for the Extraction of Hydrochlorothiazide from Human Urine. *ACS Sustain. Chem. Eng.* **2017**, *5* (5), 3775–3785.

(25) Beitollahi, H.; Hamzavi, M.; Torkzadeh-Mahani, M. Electrochemical Determination of Hydrochlorothiazide and Folic Acid in Real Samples Using a Modified Graphene Oxide Sheet Paste Electrode. *Mater. Sci. Eng. C* **2014**, *52*, 297–305.

(26) Aydoğmuş, Z. Simultaneous Determination of Aliskiren, Amlodipine and Hydrochlorothiazide in Spiked Human Plasma and Urine by High Performance Liquid Chromatography. *J. Anal. Chem.* **2015**, *70* (4), 502–509.